Hindawi Publishing Corporation
International Journal of Photoenergy
Volume 2015, Article ID 457980, 8 pages
http://dx.doi.org/10.1155/2015/457980

Research Article

Photocorrosion Mechanism of TiO_2-Coated Photoanodes

Arjen Didden,[1] Philipp Hillebrand,[2] Bernard Dam,[1] and Roel van de Krol[1,2]

[1]*Materials for Energy Conversion and Storage, Faculty of Applied Sciences, Delft University of Technology, Julianalaan 136, 2628 BL Delft, Netherlands*
[2]*Helmholtz-Zentrum Berlin für Materialien und Energie GmbH, Institute for Solar Fuels, Hahn-Meitner-Platz 1, 14109 Berlin, Germany*

Correspondence should be addressed to Roel van de Krol; roel.vandekrol@helmholtz-berlin.de

Received 10 May 2015; Accepted 13 July 2015

Academic Editor: Antoni Morawski

Atomic layer deposition was used to coat CdS photoanodes with 7 nm thick TiO_2 films to protect them from photocorrosion during photoelectrochemical water splitting. Photoelectrochemical measurements indicate that the TiO_2 coating does not provide full protection against photocorrosion. The degradation of the film initiates from small pinholes and shows oscillatory behavior that can be explained by an Avrami-type model for photocorrosion that is halfway between 2D and 3D etching. XPS analysis of corroded films indicates that a thin layer of CdS remains present on the surface of the corroded photoanode that is more resilient towards photocorrosion.

1. Introduction

CdS films have ideal band positions for photoelectrochemical water splitting [1] but one of the limiting factors is the severe photocorrosion that the films experience in aqueous media [2]. To protect CdS photoanodes from photocorrosion, the surface of the film can be modified with a catalyst that promotes the water splitting reaction, or to add a hole scavenger to the electrolyte. In both cases, the photocorrosion is suppressed through kinetic competition.

An alternative protection mechanism is to deposit a protective coating that creates a physical barrier between electrolyte and the photoactive material [3–6]. Two strategies have been reported in literature. One is to find a hole-conducting material that is stable in electrolyte and has a valence band level that is positioned between that of the photoanode and the oxygen evolution potential of water [3]. In this case, the charge carriers can easily transfer from the bulk semiconductor to the coating layer and, subsequently, into the electrolyte. An example of this is the "leaky" TiO_2/Ni films that were recently reported by Hu et al. [7]. The other strategy is to coat the photoactive material with an extremely thin layer that is thick enough to provide full protection but thin enough to enable tunneling of holes through it [4, 5].

In view of its excellent chemical stability, TiO_2 is a promising candidate as an ultrathin protection layer for CdS photoanodes. The band diagram of CdS/TiO_2 system is given in Figure 1. Because the TiO_2 valence band edge lies below the CdS level, the layer should be extremely thin in order to let holes tunnel through. Depositing such ultrathin protection layers requires a very high degree of precision and thickness control. Atomic layer deposition (ALD) is a well-suited technique for this purpose, which allows ultrathin layers of a variety of materials to be deposited by employing a sequence of self-limiting adsorption reactions. The self-limiting nature of the reactions gives homogeneous coatings with an excellent thickness control [8].

Even though coating with a protective layer does improve the stability of photoelectrodes, it often does not provide full protection. For example, Cu_2O photocathodes were found to degrade even after more than 10 nm TiO_2 had been deposited with ALD [3, 4]. Furthermore, corrosion experiments on other types of substrates that were coated with ALD films show that, in spite of the excellent conformal coverage that is normally ascribed to ALD coatings, corrosion still occurs

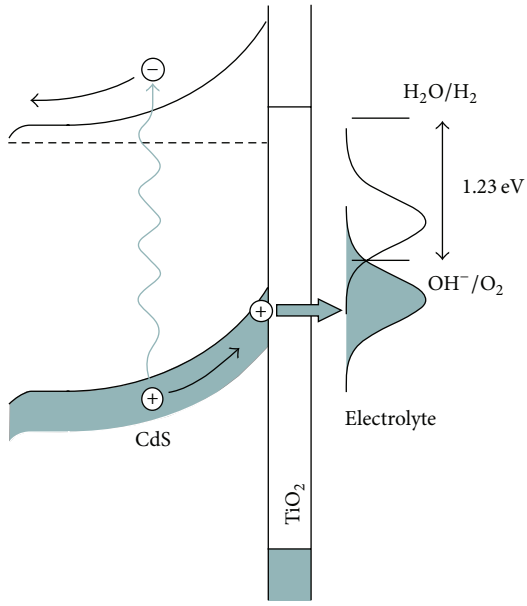

Figure 1: Band diagram of a TiO_2-coated CdS photoanode, illustrating the possibility of hole transfer by tunneling if the TiO_2 film is sufficiently thin. The redox couple's distribution of states in the electrolyte is indicated in this figure as well.

[9–11]. In order to improve the effectiveness of the coating, the photocorrosion mechanism has to be understood.

There are several ways to measure corrosion rates, for example, by soaking the samples in corrosive liquid for a given time and comparing the properties of coated and uncoated samples [10]. Yet most of these techniques only give phenomenological output and do not provide insights into the exact mechanism of (photo)corrosion. Electrochemical measurements, on the other hand, can give more detailed insights into the corrosion mechanism of coated samples over time. For example, when there is a potential difference between the substrate and the protective coating layer, the degradation of the coating can be followed by measuring changes in the potential or polarization over time [12]. Also, electrochemical impedance spectroscopy has been used to describe corrosion mechanisms [9, 11]. In this paper, we explore the photocorrosion mechanism for an n-type CdS film covered by a thin ALD-deposited TiO_2 protection layer using time-resolved photocurrent measurements. We will show that the behavior can be described with an Avrami-type model that suggests that corrosion mainly takes place in the lateral direction. Moreover, we show that the addition of a hole scavenger cannot fully suppress degradation.

2. Experimental

Polycrystalline, ~100 nm thick CdS films were deposited on FTO substrates (fluorine-doped tin dioxide, 15 Ω/sq., TEC 15, Libbey-Owens-Ford) with chemical bath deposition (CBD) according to a method described before [13]. Before CBD, the substrates were cleaned by ultrasonic rinsing in acetone and ethanol, followed by a 5 s dip in a dilute HCl solution

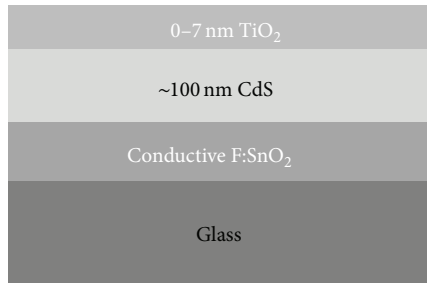

Figure 2: Sample structure of the CdS photoanodes coated with thin TiO_2 films.

(17.5%) and subsequent rinsing with ultrapure deionized water (Milli-Q, 18.2 MΩcm).

After CBD, the samples are rinsed and cleaned ultrasonically in ultrapure water (Milli-Q, 18.2 MΩ cm) to remove loose particulate matter and subsequently dipped in H_2O_2 and rinsed with ultrapure water. Prior to coating by ALD, the samples were rinsed with ultrapure water and blow-dried with nitrogen. The CdS films were coated with TiO_2 in a home-built ALD reactor. TDMAT (*tetrakis*-dimethylaminotitanium, SAFC electronic grade) and water (Milli-Q) were used as precursors for TiO_2 deposition. TDMAT was used as Ti-precursor instead of the more common precursor $TiCl_4$ to prevent formation of corrosive HCl as by-product during the ALD reaction. The deposition temperature was 200°C and the base pressure 1 Pa. All precursors were fed to the reactor by evaporation, without using a carrier gas. To ensure a sufficient vapor pressure, the TDMAT container was heated to 70°C and the supply lines were heated to 80°C to prevent condensation. Pulse times used were 3 s and 10 ms for the TDMAT and water, respectively. The TiO_2 growth rate, measured on Si wafers with *in situ* ellipsometry using a Woollam M2000 F spectroscopic ellipsometer, was 1.2 Å/cycle. After deposition, the samples were annealed at 450°C to form crystalline anatase TiO_2.

Photoelectrochemical measurements were carried out in a three-electrode cell made from Teflon, using an Ag/AgCl reference electrode and a Pt counter electrode. Solutions of KOH (Sigma Aldrich reagent grade, 0.1 M) and Na_2SO_3 (Sigma Aldrich reagent grade, 0.5 M) in water (Milli-Q) served as electrolyte. The potential was applied by a potentiostat (Princeton Applied Research, model EG&G 283), and a class AAA solar simulator (AM1.5, 1000 W/m^2, Newport Sol3A type 94023-ASR3) was used to illuminate the samples.

X-ray photoelectron spectroscopy (XPS) measurements were carried out with a Specs XR50 X-ray source (Mg Kα radiation) and a Phoibos 100 analyzer.

3. Results and Discussion

Thin TiO_2 layers were deposited on polycrystalline CdS films. The sample geometry is given in Figure 2. The polycrystalline CdS films were n-type, with a film thickness of approximately 100 nm. A more detailed description of the CdS films is given elsewhere [13].

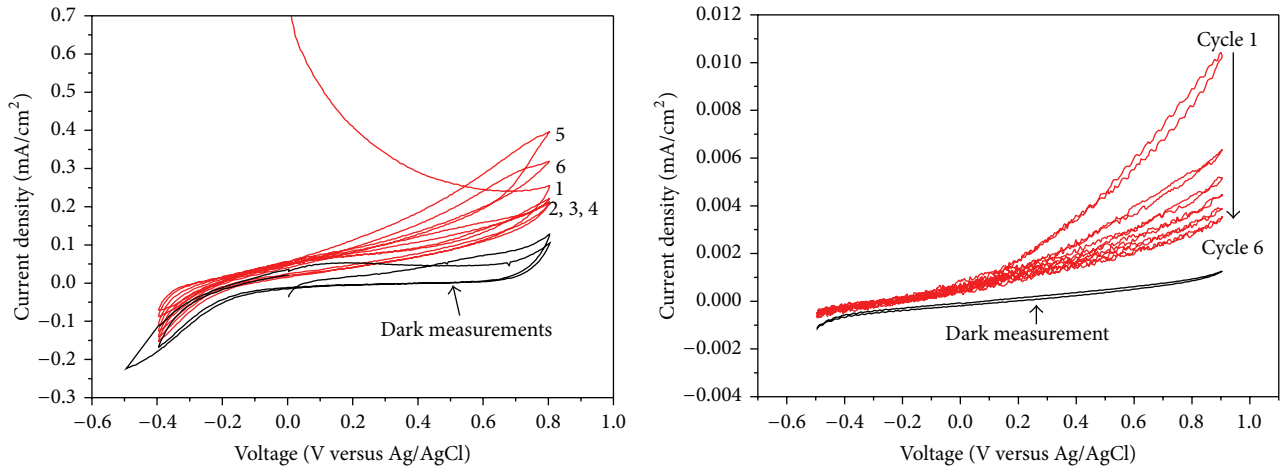

FIGURE 3: I-V curves in 0.1 M KOH solution of CdS films coated with 30 (a) and 60 (b) ALD cycles of TiO_2. Scan rates were 100 mV/s. Red lines represent photocurrent measurements and black lines dark measurements.

When we look at the I-V curves of samples coated with 30 and 60 cycles of ALD (Figures 3(a) and 3(b)) taken in KOH electrolyte in the dark and under simulated solar radiation, the first thing that stands out is that the samples are not stable over several voltage cycles when exposed to light (reference samples without ALD coating degraded too fast for meaningful I-V curves to be recorded). For the sample with 30 ALD cycles we first observe an increase in photocurrent (up to I-V cycle 5) after which the photocurrent decreases again. For the sample with 60 ALD cycles, the highest photocurrent is measured in the first I-V cycle and the photocurrent gradually decreases after each consecutive cycle. Clearly, even after 60 cycles ALD (~7 nm TiO_2 coating), the coating is not thick enough to provide sufficient protection against photocorrosion. Furthermore, the current density of the sample coated with 60 cycles is about two orders of magnitude smaller than that of the sample coated with 30 cycles. This suggests that the coating layer on top of the CdS filmblocks the current. Also for these films, the photocurrent of the coated samples is not stable during cycling.

To investigate the transient behavior of coated samples, the photocurrent was measured at a fixed potential of 0.5 V versus Ag/AgCl. Figure 4 gives a typical result of the behavior of coated samples over time. After turning on the light at $t = 0$, the current instantaneously rises to a maximum, then decreases, rises again, and finally slowly decays to zero.

The oscillatory behavior of the photocurrent can be modeled by assuming that the photocurrent is the sum of the photocorrosion and water oxidation reactions that occur simultaneously at the photoanode [14–16]:

$$\mathrm{Cd^{2+}\,(aq) + S\,(ads) + 2e^- \longleftrightarrow CdS\ (s)} \quad (E = 0.324\ \mathrm{V\ versus\ NHE\ [15]}) \tag{1}$$

$$\mathrm{2H_2O + O_2 + 4e^- \longleftrightarrow 4OH^-} \quad (E = 0.401\ \mathrm{V\ versus\ NHE}) \tag{2}$$

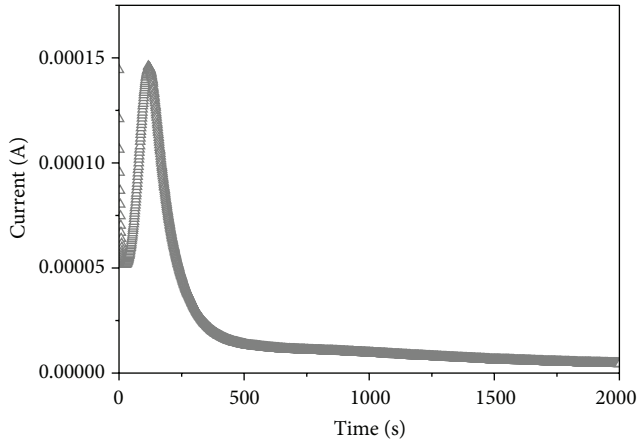

FIGURE 4: Development of current over time in 0.1 M KOH upon illumination of a CdS sample coated with 200 ALD cycles.

Photoinduced water oxidation at semiconductor electrodes has been extensively studied and to the best our knowledge has never been reported to give oscillatory behavior. We therefore attribute the photocurrent to photocorrosion of CdS (1). We can explain this behavior by assuming that corrosion is initiated from a number of defects in the coating, as schematically shown in Figure 5. These defects can be microscopic pinholes or cracks caused by incomplete surface coverage, annealing, or lattice mismatch between CdS and TiO_2 (Figure 5(a)). Starting at these defects, the CdS layer is etched way (Figures 5(b) and 5(c)). Due to the etching, the etched regions expand (Figure 5(d)), until they converge with other regions (Figure 5(e)). The etching will continue until the entire layer is consumed.

Inspection of partially corroded samples with an optical microscope (Figure 6) confirms that corrosion pits are formed in the CdS film. The large corroded areas seem to be made up of smaller, more or less circular corrosion pits

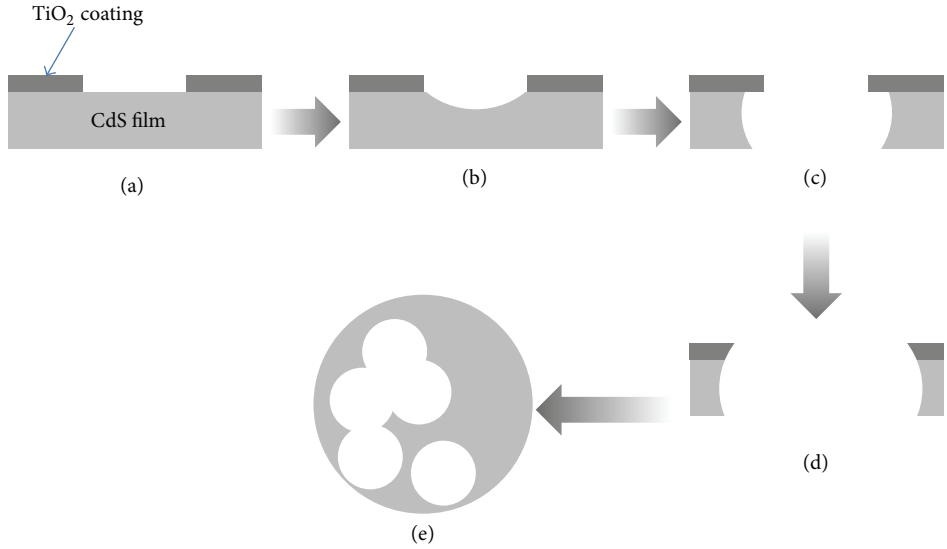

Figure 5: Schematic view of the corrosion mechanism where the corrosion starts with the presence of pinhole or crack in the pristine sample (a) at which the corrosion is initiated (b). The corrosion then expands in all directions until the substrate underneath the CdS is reached (c), after which the corrosion pit expands in lateral direction (d) until it merges with one or more neighboring corrosion pits (e).

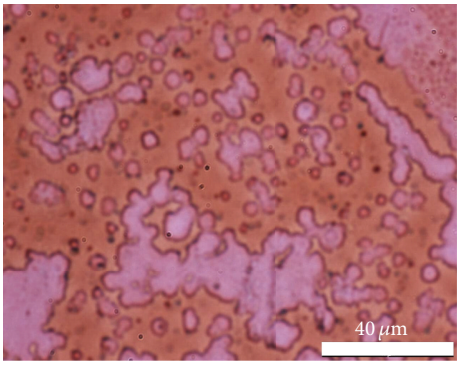

Figure 6: Optical micrograph of a CdS film coated with 60 cycles ALD after a photoelectrochemical experiment.

that have joined together. This is indeed consistent with the mechanism depicted in Figure 5.

This behavior can be translated to the observed current oscillations by assuming that the photocurrent is caused by corrosion of the film. The two holes required for every molecule of CdS that is etched away (see (1)) will contribute to the photocurrent.

The high current immediately after switching on the light is due to excitation of electron-hole pairs. But since the flux of holes to the surface is larger than the rate at which they can be consumed by chemical reactions, they accumulate near the surface. As a result, recombination increases, which leads to a decrease of the current. This transient behavior is often observed in photoelectrochemical experiments that use chopped illumination. The decrease in current resembles the discharge of a capacitor over time, where the charge of the capacitor corresponds to the number of accumulated holes. This can be expressed as the recombination current:

$$I_{\text{recomb.}} = I_0 \exp\left(-\frac{t}{\tau}\right). \quad (3)$$

In this equation, I_0 is the initial current (A), t is time (s), and τ is the time constant of the decay (s).

Since the area of the pinholes is small and the decay of the photocurrent due to recombination is fast, the contribution of photocorrosion is most likely negligible for the first transient peak at $t < 50$ s in Figure 4. Assuming that the corrosion reaction only takes place at the edges of the small pin holes, the corrosion rate will gradually increase with the size of the holes as the CdS at the edges dissolves. Larger circumferences of the holes lead to larger reactive surfaces (Figures 5(c) → 5(d)). The availability of more reactive surface will increase the photocurrent, which marks the start of the second current peak at $t > 50$ s.

This increase in photocurrent will continue until one corrosion pit converges with a second, and perhaps third pit (Figure 5(e)). When two pits meet, the point where they merge will contain no more CdS and, hence, their amount of reactive surface area will decrease. This will slow down the growth of the reactive surface until at some point it will start to decrease. This corresponds to the sharp decrease in photocurrent after the peak. As shown in Figure 4, the current decreases quickly to values below 0.05 mA/cm^2, after which the photocurrent levels off more gradually towards the end of the experiment.

This photocorrosion model strongly resembles the Avrami model for crystal growth in metals. This model predicts the fraction Φ of material converted into a new

phase (in this case, the material etched away) as a function of time t with the equation [17]

$$\Phi = 1 - \exp\left(-kt^n\right). \quad (4)$$

Here, the constant k is the product of a shape factor, the effective number of nuclei, and the direction-averaged growth rate. The exponent n is the sum of the dimension of the crystal growth process (1 for needle-like, 2 for plate-like, and 3 for 3D growth) and an integer value describing the nucleation rate (1 for constant nucleation rate, 0 for the absence of nucleation). In this model we assume that the corrosion rate in the lateral direction is constant. Furthermore, since the size of the pin holes is several orders of magnitude larger than the film thickness (micrometers versus tens of nanometers; see Figure 6), etching will mostly take place in the lateral direction and the process will most likely be 2-dimensional.

If we assume that O_2 production at the photoanode is negligible, the fraction of material that has been corroded can be described by integrating the corrosion current I_{corr}:

$$\Phi = \frac{1}{dA\rho_M N_A q} \int_0^t \frac{1}{\eta} I_{\text{corr}} dt. \quad (5)$$

In this equation, d is the thickness of the film (in m), A the total surface area of the electrode (2.82×10^{-5} m^2), ρ_M the molar density (mol/m^3), N_A Avogadro's number, q the elementary charge (C), and η the number of electrons consumed per reaction (−). Combining (4) and (5) and integration yield

$$I_{\text{corr}} = \alpha n k t^{n-1} \left(\exp\left(-kt^n\right)\right) \quad (6)$$

with

$$\alpha \equiv dA\rho_M q\eta. \quad (7)$$

The total current can be expressed as the sum of the recombination current, $I_{\text{recomb.}}$, the corrosion current, I_{corr}, and a linear equation ($at + b$) that is used to fit the sloping part of the curve that is visible at the second half of the curve:

$$I = \alpha n k t^{n-1} \left(\exp\left(-kt^n\right)\right) + I_0 \exp\left(-\frac{t}{\tau}\right) + at + b. \quad (8)$$

The fit parameters are α, n, k, τ, a, and b.

The equation was used to fit the experimental data given in Figure 4, which shows the photocurrent transient of a CdS sample coated with 200 cycles ALD in 0.1 M KOH. Figure 7 shows the best possible fit to the data.

The fit results in a value of 3.6×10^{-6} s^{-n} for k and, more importantly, an exponent n equal to 2.5. Assuming that no additional pinholes or other corrosion nuclei are formed during the corrosion process (which means that all nuclei are imperfections in the TiO_2 coating and that no other nuclei are formed), the part of the exponent that is related to the nucleation rate can be assumed to be 0. The corrosion is then partly plate-like (2-dimensional) and partly in three dimensions, which means that the layer dissolves in the lateral direction starting from the initially present pinholes.

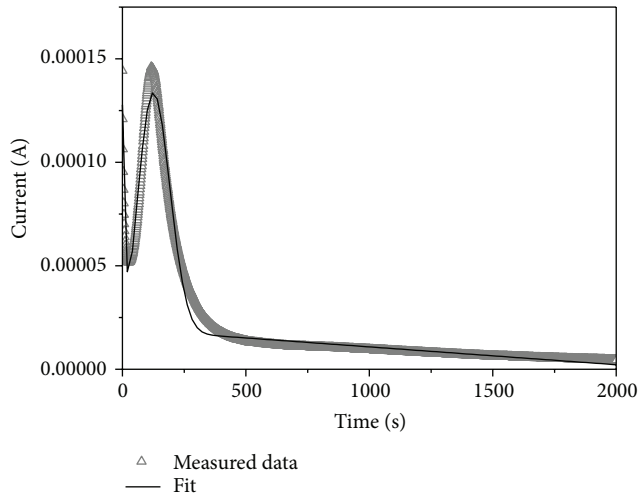

Figure 7: Photocurrent transient after turning on the light at $t = 0$ (grey triangles) and a fit of the data with (8) (black line).

The value for α is equal to 17.5 mC. From this, the film thickness d can be calculated with (5). With a CdS molar density of 33.4 kmol/m^3, a surface area of 2.82×10^{-5} m^2, and the standard values of N_A and q (6.02×10^{23} mol^{-1} and 1.6×10^{-19} C, resp.), the calculated value for the thickness d is equal to 96.6 nm, which indeed matches well with the measured film thickness of approximately 100 nm. This confirms our initial assumption that the photocurrent can be entirely attributed to photocorrosion, with negligible contribution from water oxidation.

In contrast to what the model predicts, the photocurrent does not go entirely to zero after the main current peak ($t >$ 500 s) but instead shows a linear decrease. This suggests that part of the photoactive layer remains on the FTO substrate and corrodes much slower than the rest of the CdS layer. Alternatively, part of the linearly decreasing photocurrent may be due to water oxidation at the exposed FTO surface.

To investigate this, the composition of the surface of a corroded sample has been analyzed with XPS and compared to that of the as-deposited samples (with 60 and 200 cycles of ALD, Figure 8). The as-deposited samples reveal a small but clear Ti signal. In contrast, no Ti signal can be observed for the fully corroded sample (Figure 6, bottom curve). This confirms that the TiO_2 coating is completely removed during etching. Surprisingly, however, the fully corroded sample shows no Sn signal that would indicate the presence of the underlying FTO film. This indicates that at least a few nm of CdS remains on the surface and that little or no FTO is exposed to the electrolyte. The thin CdS layer apparently is able to generate a persistent photocurrent after 500 s. This suggests that the CdS layers initially grown on the FTO are more resilient to etching. The reason for this is unknown and calls for further investigation.

Interestingly, the spectra of the as-deposited samples with both 60 and 200 ALD-TiO_2 cycles still show strong Cd and S peaks. The penetration depth of XPS is typically < 5 nm, which means that both Cd and S are present within the uppermost 5 nm of the sample. Because the deposited film is

Table 1: The table gives the atomic composition of the samples. The numbers between brackets indicate surface area of the corresponding peaks.

	As-deposited 60 c. ALD	As-deposited 200 c. ALD	Corroded 200 c. ALD
C	43.4 (35561)	41.2 (401013)	36.8 (7670)
Cd	20.7 (316291)	15.5 (282556)	16.9 (65913)
O	22.1 (44489)	31.8 (76043)	42.1 (21520)
S	11.8 (17316)	6.7 (11669)	4.2 (1556)
Ti	2.1 (11962)	4.8 (32798)	0.0 (0)
Sn	0.0 (0)	0.0 (0)	0.0 (0)

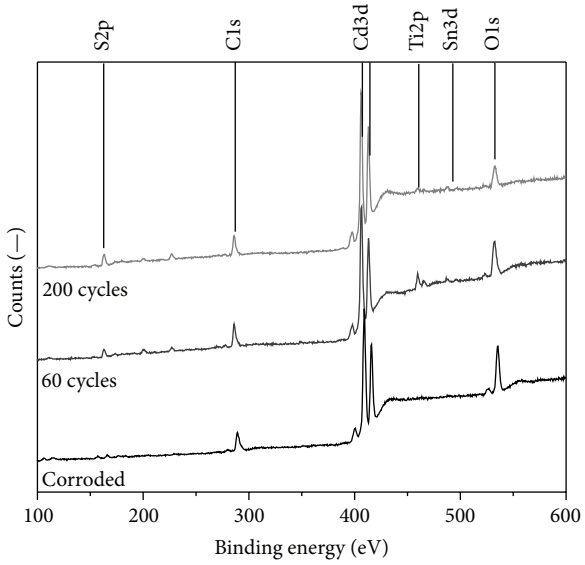

Figure 8: XPS spectra of a fully corroded sample that was originally coated with 200 cycles of ALD (1) and as-deposited samples with 60 (2) and 200 (3) cycles of ALD. The vertical lines indicate the most prominent element peaks. The spectra are offset for clarity.

much thicker than 5 nm (7 and 24 nm for 60 and 200 cycles, resp.) this means that either Cd has diffused through the TiO_2 during the thermal anneal or the TiO_2 coating is not homogeneous.

Extensive diffusion of Cd through TiO_2 is unlikely. No data on diffusion rate is available in literature, but based on the much larger ionic radius of Cd^{2+} compared to that of Ti^{4+} (95 versus 61 pm, resp. [18]), it is reasonable to assume that Cd diffusion through solid TiO_2 is very slow. The fact that we nevertheless observe a Cd signal suggests that the TiO_2 layer does not fully cover the CdS. The presence of uncovered CdS, possibly in the form of pin holes, is indeed consistent with the photocorrosion that we observed and described above.

The molar fractions calculated from the XPS data (given in Table 1) indicate that the concentration of O atoms at

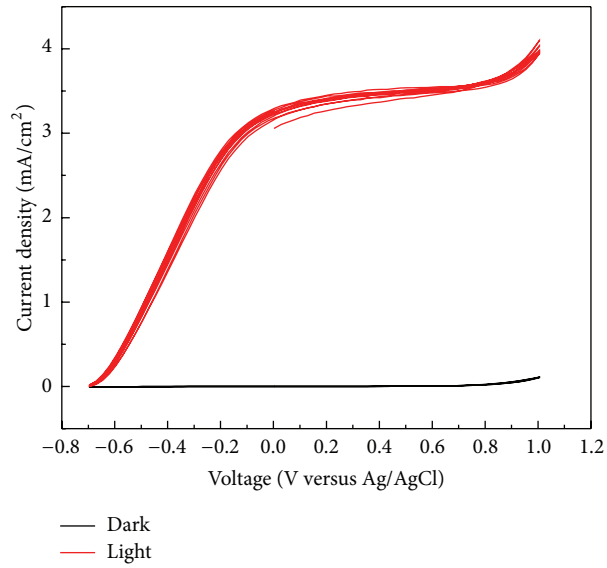

Figure 9: *IV* curves of uncoated CdS in Na_2SO_3 in dark conditions and under solar radiation, measured at scan rates of 100 mV/s.

the surface is more than 2 times higher than the concentration of Ti, whereas the concentration of S is lower than that of Cd. This strongly suggests that other components such as $CdSO_4$, CdS_2O_3, CdO, or $Cd(OH)_2$ are present at the surface due to partial oxidation or hydroxylation of the CdS. Furthermore, the broadness of the C1s peak, with contributions at above 287 eV, indicates that carbon impurities are present in the form of carbonates.

An alternative protection strategy is to use an electrolyte that reacts with the holes on a time scale that is much faster than the CdS oxidation reaction. This would kinetically stabilize the photoanode. Na_2SO_3 was used as such a "hole scavenger" because the oxidation of sulfite to sulfate is a two-electron redox reaction which is known to be much faster than the four-electron water oxidation reaction [19].

The effect of using Na_2SO_3 electrolyte rather than KOH becomes clear when comparing the *IV* curves in Figure 9 with the *IV* curves of a sample in KOH given in Figure 3. The sample in KOH shows instability of the photocurrent upon cycling, whereas the sample in Na_2SO_3 shows little or no decay after cycling.

Even though the Na_2SO_3 stabilizes the sample during the *IV* measurements, long-term experiments (>40 minutes) show that even with a hole scavenger present the photocurrent decreases over time. This is clearly visible in Figure 10, where the photocurrent (under chopped AM1.5 illumination) of a CdS sample in Na_2SO_3 electrolyte is given (the insert shows the photocurrent over a 1-minute time span).

Assuming that the absorption of incident light by the CdS is linearly dependent on the layer thickness, the corrosion rate can be estimated from the time-dependent decrease of photocurrent and the dependence of the photocurrent on the amount of absorbed light. The decay in photocurrent is approximately 0.12 (μA/cm^2)/s. Assuming that an initial film thickness of ~100 nm gives a photocurrent of 3.2 mA/cm^2

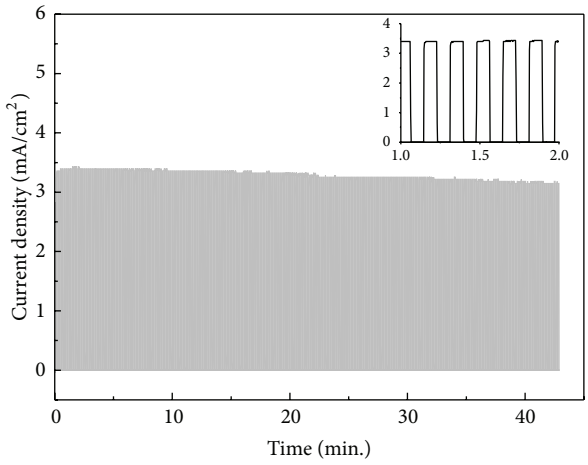

FIGURE 10: Current in time for an uncoated CdS sample in Na_2SO_3 electrolyte at 0.5 V versus Ag/AgCl.

(Figure 9), the decay in photocurrent corresponds to a dissolution rate of approximately 12.5 pmol/cm^2/s, or 4 pm/s. The sulfite oxidation rate at $t = 0$, assuming that all photocurrent is used for sulfite oxidation, is 36 nmol/cm^2/s. Two assumptions have to be made for the estimated rates to be valid: (a) the change in Na_2SO_3 concentration at the sample surface is negligible and (b) the efficiency of light absorption, charge separation, and charge transfer to the electrolyte remains constant. The reduction of sulfite concentration, calculated by integrating the photocurrent over time and subtracting this from the initial concentration, is <1%, which is indeed negligible. As the anode material does not change but merely dissolves slowly over time, the second assumption is also likely to hold. Hence, we conclude that the sulfite oxidation rate is ~3 orders of magnitude faster than the photocorrosion rate. This is clearly insufficient to guarantee long-term stability of the CdS photoanode.

4. Conclusion

Although films deposited with ALD are supposed to be highly conformal, we find that thin ALD-TiO_2 films are not able to protect CdS films against photocorrosion in aqueous KOH solutions. The corrosion starts from pinholes in the TiO_2 protection layer where the CdS is in direct contact with the electrolyte. The observed photocurrents are mainly due to corrosion, as opposed to water oxidation. The photocurrent shows a well-defined and reproducible oscillation peak that can be fitted with an Avrami-type model that suggests a partly lateral (2D), partly 3D photocorrosion mechanism of the CdS film.

XPS analysis of the samples confirms that the samples are indeed not completely coated with TiO_2 and that a mixture of CdS and partially oxidized or hydroxylated phases (e.g., $Cd(OH)_2$) are present at the surface. The XPS analysis also revealed that a thin layer of CdS remains present at the surface, even after prolonged exposure to light. The reason for the high photochemical stability of the bottom part of the CdS layer is not fully understood.

Using Na_2SO_3 as a hole scavenger greatly improves the stability of the CdS films. It does not, however, completely solve the photocorrosion problems of CdS. In the end, having a protective layer that (a) can conduct holes, (b) is stable in aqueous solutions, and (c) is completely free of pinholes will provide a more lasting protection.

Conflict of Interests

The authors declare that there is no conflict of interests regarding the publication of this paper.

Acknowledgments

This research is financially supported by the Thin Film Nanomanufacturing Program of the Dutch Technology Foundation STW (Project 10016). The authors would like to thank Lennard Mooij for stimulating discussions.

References

[1] M. F. Finlayson, B. L. Wheeler, N. Kakuta et al., "Determination of flat-band position of CdS crystals, films, and powders by photocurrent and impedance techniques. Photoredox reaction mediated by intragap states," *Journal of Physical Chemistry*, vol. 89, no. 26, pp. 5676–5681, 1985.

[2] D. Meissner, R. Memming, and B. Kastening, "Photoelectrochemistry of cadmium sulfide. 1. Reanalysis of photocorrosion and flat-band potential," *The Journal of Physical Chemistry*, vol. 92, no. 12, pp. 3476–3483, 1988.

[3] A. Paracchino, V. Laporte, K. Sivula, M. Grätzel, and E. Thimsen, "Highly active oxide photocathode for photoelectrochemical water reduction," *Nature Materials*, vol. 10, no. 6, pp. 456–461, 2011.

[4] A. Paracchino, N. Mathews, T. Hisatomi, M. Stefik, S. D. Tilley, and M. Grätzel, "Ultrathin films on copper(I) oxide water splitting photocathodes: a study on performance and stability," *Energy and Environmental Science*, vol. 5, no. 9, pp. 8673–8681, 2012.

[5] K. Yu, X. Lin, G. Lu, Z. Wen, C. Yuan, and J. Chen, "Optimized CdS quantum dot-sensitized solar cell performance through atomic layer deposition of ultrathin TiO_2 coating," *RSC Advances*, vol. 2, no. 20, pp. 7843–7848, 2012.

[6] M. Shalom, S. Dor, S. Rühle, L. Grinis, and A. Zaban, "Core/CdS quantum dot/shell mesoporous solar cells with improved stability and efficiency using an amorphous TiO_2 coating," *Journal of Physical Chemistry C*, vol. 113, no. 9, pp. 3895–3898, 2009.

[7] S. Hu, M. R. Shaner, J. A. Beardslee, M. Lichterman, B. S. Brunschwig, and N. S. Lewis, "Amorphous TiO_2 coatings stabilize Si, GaAs, and GaP photoanodes for efficient water oxidation," *Science*, vol. 344, no. 6187, pp. 1005–1009, 2014.

[8] R. L. Puurunen, "Surface chemistry of atomic layer deposition: a case study for the trimethylaluminum/water process," *Journal of Applied Physics*, vol. 97, pp. 121301–121353, 2005.

[9] B. Díaz, E. Härkönen, V. Maurice et al., "Failure mechanism of thin Al_2O_3 coatings grown by atomic layer deposition for corrosion protection of carbon steel," *Electrochimica Acta*, vol. 56, no. 26, pp. 9609–9618, 2011.

[10] X. Du, K. Zhang, K. Holland, T. Tombler, and M. Moskovits, "Chemical corrosion protection of optical components using atomic layer deposition," *Applied Optics*, vol. 48, no. 33, pp. 6470–6474, 2009.

[11] C. X. Shan, X. Hou, and K.-L. Choy, "Corrosion resistance of TiO_2 films grown on stainless steel by atomic layer deposition," *Surface and Coatings Technology*, vol. 202, no. 11, pp. 2399–2402, 2008.

[12] G. Bech-Nielsen, M. Jaskula, I. Chorkendorff, and J. Larsen, "The initial behaviour of freshly etched copper in moderately acid, aerated chloride solutions," *Electrochimica Acta*, vol. 47, no. 27, pp. 4279–4290, 2002.

[13] A. Didden, H. Battjes, R. MacHunze, B. Dam, and R. Van De Krol, "Titanium nitride: a new Ohmic contact material for n-type CdS," *Journal of Applied Physics*, vol. 110, no. 3, Article ID 033717, 2011.

[14] D. Meissner, R. Memming, and B. Kastening, "Photoelectrochemistry of cadmium sulfide. 1. Reanalysis of photocorrosion and flat-band potential," *Journal of Physical Chemistry*, vol. 92, no. 12, pp. 3476–3483, 1988.

[15] A. J. Bard and M. S. Wrighton, "Thermodynamic potential for the anodic dissolution of n-type semiconductors: a crucial factor controlling durability and efficiency in photoelectrochemical cells and an important criterion in the selection of new electrode/electrolyte systems," *Journal of the Electrochemical Society*, vol. 124, no. 11, pp. 1706–1710, 1977.

[16] D. J. Fermin, E. A. Ponomarev, and L. M. Peter, "A kinetic study of CdS photocorrosion by intensity modulated photocurrent and photoelectrochemical impedance spectroscopy," *Journal of Electroanalytical Chemistry*, vol. 473, no. 1-2, pp. 192–203, 1999.

[17] M. Avrami, "Kinetics of phase change. II Transformation-time relations for random distribution of nuclei," *The Journal of Chemical Physics*, vol. 8, no. 2, pp. 212–224, 1940.

[18] Y.-M. Chiang, D. P. Birnie, and W. D. Kingery, *Physical Ceramics: Principles for Ceramic Science and Engineering*, John Wiley & Sons, 1996.

[19] T. Inoue, T. Watanabe, A. Fujishima, K. Honda, and K. Kohayakawa, "Suppression of surface dissolution of Cds photoanode by reducing agents," *Journal of Electroanalytical Chemistry*, vol. 124, no. 5, pp. 719–722, 1977.